

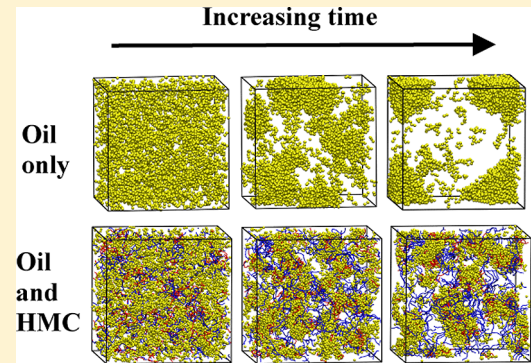
Simulation Study of Hydrophobically Modified Chitosan as an Oil Dispersant Additive

Steven W. Benner,[†] Vijay T. John,[‡] and Carol K. Hall*,[†]

[†]Department of Chemical and Biomolecular Engineering, North Carolina State University, Raleigh, North Carolina 27695-7905, United States

[‡]Department of Chemical and Biomolecular Engineering, Tulane University, New Orleans, Louisiana 70118, United States

ABSTRACT: Hydrophobically modified chitosan (HMC) is being considered as a possible oil dispersant additive to reduce the volume of dispersant required in oil spill remediation. We present the results of discontinuous molecular dynamics (DMD) simulations intended to determine how the HMC architecture affects its ability to prevent oil aggregation. The HMCs have a comb copolymer architecture with hydrophobic side chains (modification chains) of various lengths (5–15 spheres) to represent alkane chains that are attached to the chitosan backbone. We calculated the oil's solvent accessible surface area (SASA), aggregate size distribution, and aggregate asymmetry at various values of the HMC modification chain length, modification density, and concentration to determine HMC efficacy. HMCs with long modification chains result in larger oil SASA than HMCs with short modification chains. For long modification chains, there is no increase in oil SASA with increasing modification density above a saturation value. The size distribution of the oil aggregates depends on the modification chain length; systems with long modification chains lead to large aspherical aggregates, while systems with short modification chains lead to small tightly packed aggregates. A parametric analysis reveals that the most important factor in determining the ability of HMCs to prevent oil aggregation is the interaction between the HMC's modification chains and the oil molecules, even when using short modification chains. We conclude that HMCs with long modification chains are likely to be more effective at preventing oil aggregation than HMCs with short modification chains, and that long modification chains impede spherical oil droplet formation.



INTRODUCTION

Oil spills have caused major environmental disasters over the past 50 years, the two most notable being the Exxon Valdez spill in 1989 and the recent Deepwater Horizon spill in 2010.^{1,2} Dispersants were used following the Deepwater Horizon spill in an effort to prevent oil slicks, and to promote the natural degradation of oil by ocean bacteria,^{1,3,4} but there was significant debate over their toxicity and effectiveness. Dispersants such as Corexit 9500A work by lowering the interfacial tension between oil and water and hence promote mixing, a process that is assisted by mechanical input from wind or wave energy. This results in the formation of much smaller oil droplets than would otherwise have occurred.⁵ If there was a way to stabilize the small oil droplets before they have the chance to re-coalesce, this would enhance the dispersants' effectiveness because it would increase the surface area of oil exposed to hydrocarbon-degrading bacteria.^{3,6} In this paper, we consider a viable option for a biocompatible oil dispersant additive, hydrophobically modified chitosan (HMC), which has been suggested to be both environmentally friendly and effective at preventing oil coalescence.

We are investigating the efficacy of HMCs as an oil dispersant additive to stabilize small oil droplets in water for use in oil spill remediation to potentially reduce the amount of

dispersant required. Chitosan is a linear polysaccharide composed of a mixture of D-glucosamine and N-acetyl-D-glucosamine monomers derived from chitin, a naturally occurring polymer found in the exoskeletons of ocean crustaceans such as crabs and shrimp.^{7,8} Chitosan can be hydrophobically modified through a reductive amination reaction, giving it an amphiphilic functionality.⁹ Previous studies have explored the behavior of chitosan and hydrophobically modified chitosan in applications such as drug delivery,^{7,10} tissue engineering,¹¹ gelation and network formation,^{12–14} and flocculating agents for oil/water emulsions.^{15–17} The idea of using HMCs as oil stabilizers was introduced by Venkataraman and co-workers.¹⁸ In their experiments, chitosan was hydrophobically modified with alkane chains, added to a mixture of crude oil, Corexit, and water, and then thoroughly mixed. The aggregation of the crude oil was monitored over time and compared to a control sample without HMCs.¹⁸ Corexit was found to be effective at breaking up the oil into small droplets but was not effective at preventing droplet re-coalescence; after only 10 min of settling

Received: February 2, 2015

Revised: May 5, 2015

time, nearly all of the oil had coalesced into a single aggregate.¹⁸ Addition of HMCs to the system prevented aggregation for the duration of their study (30 min).¹⁸ Venkataraman and co-workers speculated that HMCs anchored into the oil droplets via the hydrophobic modification chains, leaving the chitosan to wrap around the exterior of the droplets, therefore preventing oil re-coalescence through a combination of electrostatic and steric repulsion.¹⁸

The role of oil stabilizers is very similar to that of copolymer compatibilizers; both are used to prevent separation of immiscible phases. From a modeling standpoint, the HMCs can be thought of as comb copolymers, with chitosan being the comb backbone and alkane chains being the comb “teeth”. A number of studies have compared the behavior of comb copolymers to linear copolymers at the interface between immiscible polymer blends.^{19–21} Lyatskaya et al. compared the behavior of comb and diblock copolymers, and concluded that long comb copolymers with multiple teeth more effectively compatibilize an interface than short diblocks.²⁰ Gersappe et al. determined that combs with fewer long teeth located an interface more effectively than combs with many short teeth, and that comb copolymers oriented themselves at an interface more readily than multiblock copolymers of similar composition.²¹ Numerous studies have focused on the role played by comb copolymer architecture in compatibilizing an interface.^{22–24} Israels et al. showed that increasing the number and length of the “teeth” in a comb copolymer resulted in a reduction in the interfacial tension between two immiscible phases.²³ Potemkin et al. concluded that comb copolymers with long side chains undergo spontaneous bending of the backbone at an interface; this effect was significantly less pronounced as the side chain length was decreased.²⁴ Simulation studies have been used to look at how the architecture of comb copolymers affects their intramolecular interactions and conformation. Vasilevskaya et al. showed that increasing the backbone length of a comb copolymer with attractive side chains leads to an increased number of intramolecular hydrophobic domains at a set grafting density.²⁵ Other simulation studies have analyzed the orientation of copolymers at the interface between two immiscible phases and their ability to prevent phase separation^{26–28} but focused mainly on linear copolymers.

The goal of our research is to understand how the architecture of an HMC affects its ability to prevent oil aggregation with a view toward using HMCs for oil spill remediation. Simulations provide us with a molecular-level perspective on the interaction between HMCs and oil that cannot be obtained through experiment alone. Although the experimental work of Venkataraman and co-workers on HMCs has given good insight into the ability of HMCs to prevent oil coalescence, a number of questions remain such as the following. How does the length of the hydrophobic modification chains or the number of modification chains along the chitosan backbone (modification density) affect the efficacy of HMCs as oil stabilizers? What concentration of HMCs is necessary for oil droplet stabilization? What are the mechanisms by which HMCs stabilize oil droplets and how are they affected by the HMC architecture? What role does the chitosan backbone play in preventing oil droplets from aggregating? Answering these questions could lead to optimum HMC architectures for different types of oil spills and lower demand for oil dispersants.

In this paper, we present the results of discontinuous molecular dynamics (DMD) simulations designed to determine how different HMC architectures and concentrations affect their ability to prevent oil aggregation. DMD is a fast alternative to traditional molecular dynamics (MD) that allows simulations of large systems of molecules at long time scales.²⁹ The system contains two species: HMCs modeled as comb copolymers with a polar chitosan backbone and hydrophobic “teeth” and oil molecules modeled as short linear chains. Both the oil and chitosan molecules consist of chains of square-well and square-shoulder spheres. Water is modeled implicitly in all simulations, making the square-well and square-shoulder interaction potentials of mean force. Simulations are performed at various values of the modification chain length, modification density (percentage of chitosan backbone spheres containing modification chains), and overall HMC concentration. To determine how these parameters affect the HMCs’ ability to prevent oil aggregation and the mechanism by which this is effected, we monitor the oil’s solvent accessible surface area (SASA) and the number, size, and shape of oil aggregates over the course of the simulations. The oil’s SASA gives a measure of how much oil surface area would be exposed to ocean bacteria, leading to natural degradation. The oil aggregate size distribution indicates if the HMCs are preventing the oil from coalescing, therefore acting as an effective stabilizer. The shape of the oil aggregates is determined by calculating their asphericity, where the more aspherical the oil aggregates become, the more surface area is exposed to bacteria.

Highlights of our results are the following. Simulations started from a random initial configuration of HMC and oil chains lead to the formation of oil aggregates which are stabilized by HMCs. In systems containing HMCs with lower modification densities, the chitosan backbones form a network with each other and the modification chains penetrate into the oil aggregates, holding them in place and decreasing the rate of aggregation. In systems containing HMCs with higher modification densities, the modification chains form both intrachain and interchain hydrophobic clusters and penetrate into oil aggregates while the chitosan backbones remain on the exterior of the aggregates. HMCs with a few long modification chains were slightly more effective at preventing oil coalescence than HMCs with many short modification chains, even with the same total number of modification spheres. Finally, analysis of the contributions of the interaction energies between different types of spheres showed that the attractive interaction between the modification chains and the oil chains was the dominant interaction governing the HMC behavior, and that excluded volume interactions were not important in determining the effectiveness of HMCs even at high HMC volume fractions.

■ MODEL AND METHOD

All species in the system are modeled as flexible chains of spheres. Oil molecules are modeled as linear five-sphere chains where each sphere represents three carbons. We represented the oil with C15 alkanes based on an EPA study showing that these are one of the most common alkanes found in crude oil samples.³⁰ HMCs are modeled as comb copolymers with a 50-sphere chitosan backbone and modification chain lengths ranging from 5 to 15 spheres, where each modification sphere represents three carbon atoms and their corresponding hydrogen atoms (consistent with our alkane coarse-graining) and each chitosan sphere represents a glucosamine monomer. The length of the chitosan chain was chosen to be 50 spheres,

making it significantly longer than the alkane chains but not so long that we would have to simulate extremely large systems. We should point out that the chitosan backbone length in the experiments of Venkataraman and co-workers was much longer (300–1200 monomers); however, their crude oil samples also contained significantly larger hydrocarbons than C15 alkanes. The modification density, which is the percentage of chitosan backbone spheres containing modification chains, was 4, 12, or 20%. Diagrams illustrating the architecture of the HMCs used in the simulations can be seen in Figure 1. The sphere diameter,

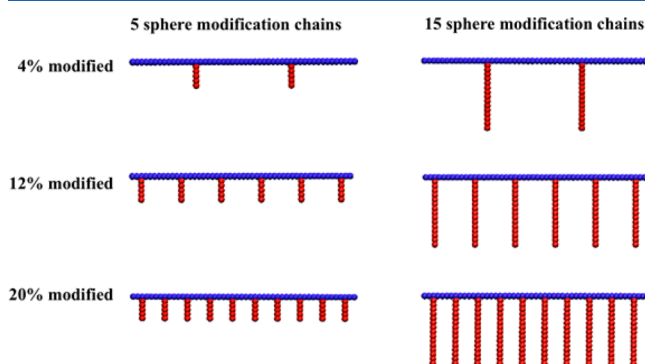


Figure 1. Schematic diagram showing the different architecture HMCs used in simulations of systems containing HMCs and oil.

σ , for all species in the system is 1.0, and the bond length between adjacent spheres on the same chain is allowed to fluctuate between $\sigma(1 + \delta)$ and $\sigma(1 - \delta)$, where $\delta = 0.01$, making the spheres tangent. If adjacent spheres reach the maximum or minimum bond length, they hit an infinite repulsive potential that bumps them back to within the allowed bond distance.^{31,32} Stiffness is incorporated into these chains using “pseudobonds” in which the minimum and maximum angles that can form between next nearest neighboring spheres along the chain are set to 122 and 180°, respectively, for the chitosan backbone and 90 and 180°, respectively, for the modification and oil chains. The chitosan backbone is stiffer than that of the alkane chains for two reasons: (1) to emulate the rigidity of a chitosan molecule and (2) to mimic the electrostatic repulsion that occurs between the cationic chitosan monomers in slightly acidic conditions. The stiffness of the oil and modification chains is maintained by a set of pseudobonds to mimic the stiffness of real alkane chains, and to prevent the oil and modification chains from collapsing in an unrealistic manner.

Interactions between spheres are modeled using square-well or square-shoulder potentials depending on whether the interaction is attractive or repulsive. The potential energy between spheres of type i and j , $U_{ij}(r)$, as a function of distance between the spheres, r , is given by the following potentials:

$$U_{ij}(r) = \begin{cases} \infty & \text{if } r \leq \sigma \\ \epsilon_{ij} & \text{if } \sigma < r \leq \lambda\sigma \\ 0 & \text{if } r > \lambda\sigma \end{cases} \quad (1)$$

where ϵ_{ij} is the interaction energy between spheres i and j and the square-well or square-shoulder width is taken to be $\lambda\sigma = 1.75$. Table 1 lists the interaction energies between each type of sphere in the system. Negative values of the interaction energy represent attractions, and positive values represent repulsions. The energies were chosen to mimic the types of interactions

Table 1. Interaction Energies between Each Type of Sphere

	chitosan	modification	oil
chitosan	-0.25	+0.5	+0.5
modification		-0.5	-0.5
oil			-0.5

expected in a system of polar and nonpolar molecules in water. Water is modeled implicitly in all simulations, making interaction energies between all spheres potentials of mean force in water. Chitosan, being polar, preferably interacts with itself over hydrocarbons. Therefore, the chitosan spheres are attracted to each other but repelled by all other spheres in the system. The hydrophobic modification chains and the oil molecules represent alkanes, and therefore are attracted to each other and repelled by chitosan. The strength of attraction between chitosan spheres is half that of the attractive interactions between hydrophobic groups to help keep the chitosan backbone extended, as it would be in the presence of water molecules. The attractive energy between chitosan monomers is weaker than the attractive energy between modification spheres, and between oil spheres, so as to prevent the chitosan backbone from collapsing on itself, but it is strong enough to encourage association with other chitosan molecules.

Details of the simulation conditions are the following. The packing fraction, $\eta = \pi N\sigma^3 / 6V$, is set to $\eta = 0.05$, where N is the total number of spheres in the system and V is the volume of the simulation box. The packing fraction was kept low to emulate a dilute system of oil in water. The three system compositions considered in the simulations are HMC volume fractions (ϕ_{hmc}) of 0.5, 0.35, and 0.2, where ϕ_{hmc} is the total volume of the HMC spheres divided by the total volume of all the spheres in the system. Systems with $\phi_{hmc} = 0.5$ contain approximately 6000 HMC spheres and 6000 oil spheres, systems with $\phi_{hmc} = 0.35$ contain approximately 4200 HMC spheres and 7800 oil spheres, and systems with $\phi_{hmc} = 0.2$ contain approximately 2400 HMC spheres and 9600 oil spheres.

DMD simulations were used in place of traditional molecular dynamics (MD) to increase the speed of the simulations while still capturing the fundamental behavior of the system.³³ Unlike traditional MD simulations, which numerically solve Newton's equations of motion every time step, DMD is an event driven technique.²⁹ The DMD simulation algorithm searches for the soonest-to-occur event (collision between spheres), advances the time to the point that the collision occurs, and analytically calculates the new particle positions and velocities after the collision.²⁹ An event occurs any time a particle reaches a discontinuity in the interaction potential as a function of separation distance such as at the boundary of a hard sphere, square-well, or square-shoulder potential. Because the method is event driven, a collision occurs every time step, avoiding the need to recalculate collision dynamics multiple times before particles are within the interaction distance of each other. Following a collision, the particles in the simulation move linearly until their next collision occurs.

The simulations began with a random initial configuration of oil and HMCs. The temperature of the system was controlled using an Andersen thermostat, where the average system reduced temperature is $T^* = k_b T / |\epsilon_{12}|$, where ϵ_{12} is the interaction energy between spheres of type 1 and type 2 (type refers to whether the sphere is a chitosan sphere, modification sphere, or oil sphere). In the Andersen thermostat, the

temperature is regulated using “ghost collisions” where a sphere in the system is randomly chosen to collide with a “ghost” sphere to maintain the Maxwell–Boltzmann velocity distribution around the desired temperature.³⁴ The first 150 million collisions of the simulation were run at a high temperature of $T^* = 8.0$ to equilibrate the system, and remove any artifacts that might arise from the choice of the initial configuration. Following the initial high-temperature portion of the simulation, the temperature was dropped by $T^* = 0.1$ every million collisions until a temperature of $T^* = 5.0$ was reached. Following this cooling, an even slower cooling procedure was performed, lowering the temperature by $T^* = 0.01$ every million collisions until the desired temperature of $T^* = 1.3$ was achieved. The rate of cooling was slowed as the set temperature was approached to allow gradual aggregation of the oil molecules. A gradual cooling procedure also more accurately represents reality, as the temperature of a system cannot suddenly drop without passing through intermediate temperatures. The temperature was held constant at $T^* = 1.3$ for the duration of the simulation (up to 2 billion collisions). A set temperature of $T^* = 1.3$ was used because it was the highest temperature at which oil molecules aggregated using the interaction energies discussed previously. At a temperature of $T^* = 1.2$, aggregation occurred rapidly and was not a gradual process over time, while at a temperature of $T^* = 1.4$ minimal aggregation was observed by the end of the simulation. We chose a temperature that allowed the oil aggregation to occur over the course of hundreds of millions of collisions because we felt that this allowed the HMCs to have sufficient time to interact with the oil. Another way to equilibrate the system would have been to only include the oil molecules in the high temperature stage, and add chitosan after the set temperature was reached. However, this might have made it harder for the chitosan to efficiently break out of its initial configuration at low temperatures. It might have also led to the formation of different equilibrium structures because oil aggregation would have already begun by the time HMCs were added. We plan to investigate this phenomenon in future work to determine how the addition of HMCs at different times affects the system equilibrium, giving insight into the importance of response time to HMC efficacy.

The efficacy of the HMCs as oil stabilizers was measured in a number of ways. First, the oil's solvent accessible surface area

(SASA) was measured using a built-in SASA function in the visual molecular dynamics (VMD) software throughout the course of the simulation to observe the overall extent of aggregation. The SASA includes (1) the area on the exterior of oil aggregates (which would be in contact with water if there had been explicit solvent) and (2) the area on the exterior of the oil aggregates that is in contact with those modification chains that lie on the exterior of the oil aggregates. The SASA was measured by removing all HMCs from the simulation box, and rolling a probe sphere of diameter 1.4 around the surface of the oil molecules. The probe sphere was chosen to be larger than the oil sphere diameter to prevent voids in the middle of aggregates (caused by removing HMC) from significantly adding to the SASA. To confirm that we selected an appropriate probe sphere size, we measured the oil SASA without removing the modification spheres present in the middle of oil aggregates for systems with the highest concentration of modification spheres. Doing this eliminated the possibility of artificial pores being present in the middle of the aggregates. The oil SASA only decreased by 4%, showing that our choice of probe size eliminated nearly all SASA contributions from the interior of the oil aggregates.

Second, we calculated the percent increase in oil SASA for various HMC architectures over systems without HMCs present. The percent increase in the oil SASA is given by

$$\% \text{ increase in oil SASA} = \left(\frac{\text{SASA}_{\text{HMC}} - \text{SASA}_{\text{noHMC}}}{\text{SASA}_{\text{noHMC}}} \right) \times 100 \quad (2)$$

where SASA_{HMC} is the oil SASA with HMCs present and $\text{SASA}_{\text{noHMC}}$ is the oil SASA without HMCs present. The number and size of the oil aggregates was also calculated at various time points to determine if the HMCs could prevent aggregation and to give insight into the mechanism of aggregation. These quantities measure how effectively the HMCs prevent oil aggregates from coalescing over time.

Third, we analyzed the shape of the oil aggregates to determine how the HMC architecture affected the ability of oil to form small droplets. The aggregate shape was characterized in terms of its asphericity.^{35,36} This method involves calculating the principal components of the gyration tensor, S , for each oil aggregate

$$\mathbf{S} = \frac{1}{N} \begin{pmatrix} \sum_i (x_i - x_{\text{cm}})^2 & \sum_i (x_i - x_{\text{cm}})(y_i - y_{\text{cm}}) & \sum_i (x_i - x_{\text{cm}})(z_i - z_{\text{cm}}) \\ \sum_i (x_i - x_{\text{cm}})(y_i - y_{\text{cm}}) & \sum_i (y_i - y_{\text{cm}})^2 & \sum_i (y_i - y_{\text{cm}})(z_i - z_{\text{cm}}) \\ \sum_i (x_i - x_{\text{cm}})(z_i - z_{\text{cm}}) & \sum_i (y_i - y_{\text{cm}})(z_i - z_{\text{cm}}) & \sum_i (z_i - z_{\text{cm}})^2 \end{pmatrix} \quad (3)$$

where x_i , y_i , and z_i are the coordinates of each oil sphere, i , in the aggregate, x_{cm} , y_{cm} , and z_{cm} are the coordinates of the aggregate's center of mass, and N is the total number of oil spheres in the aggregate. The eigenvalues of the gyration tensor λ_1 , λ_2 , and λ_3 are the principal components of the radius of gyration, R_g , defined by

$$R_g^2 = \lambda_1 + \lambda_2 + \lambda_3 \quad (4)$$

where λ_1 , λ_2 , and λ_3 are the eigenvalues of the gyration tensor. These principal components are then used to calculate the oil aggregate asphericity, A , defined as

$$A = \frac{(\lambda_1 - \lambda_3)^2 + (\lambda_2 - \lambda_3)^2 + (\lambda_1 - \lambda_2)^2}{2(\lambda_1 + \lambda_2 + \lambda_3)^2} \quad (5)$$

where $\lambda_1 \geq \lambda_2 \geq \lambda_3$. The asphericity has a minimum value of 0 for perfectly spherical aggregates and a maximum value of 1 for completely linear aggregates. The radius of gyration and

asphericity data were averaged over the final 100 million collisions of the simulations (with data recorded every 10 million collisions) and over five simulation replicates.

All of the previously mentioned analysis techniques were performed on oil aggregates in systems with and without HMCs to determine the impact of HMCs on oil aggregation. Error bars for all quantities calculated represent the standard deviation from the average of each data point over three to five replicates.

RESULTS AND DISCUSSION

Snapshots of the intermediate and final configurations in a simulation of 4% modified HMCs with 15-sphere modification chains are compared to snapshots at the same time points in a simulation containing oil only in Figure 2. Parts a and b of

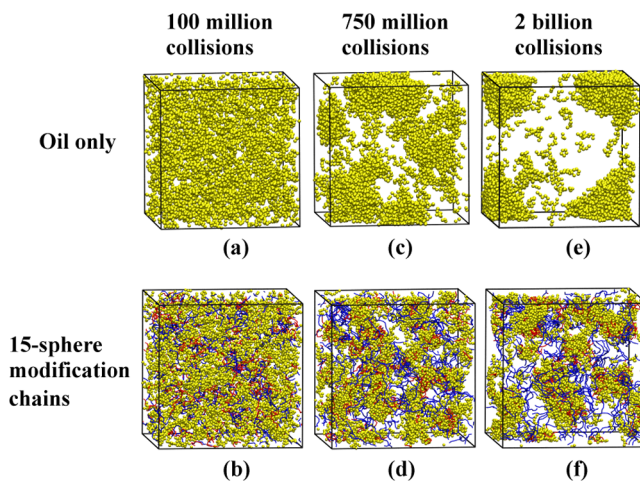


Figure 2. Snapshots of oil aggregation during simulations of systems containing oil only and oil + 4% modified HMCs with 15-sphere modification chains where $\phi_{\text{hmc}} = 0.5$. Chitosan spheres are blue, modification spheres are red, and oil spheres are yellow.

Figure 2 show system configurations with and without HMCs at 100 million collisions during the initial high temperature ($T^* = 8.0$) portion of the simulations when the system is randomized. Parts c and d of Figure 2 show both systems at 750 million collisions after the set temperature of $T^* = 1.3$ has been reached. At this point, aggregation had occurred in each system; however, the system without HMCs aggregated significantly more than the system with HMCs. At the end of the simulations (2 billion collisions), the oil-only system formed a single large aggregate, as can be seen in Figure 2e. Note that, although there appear to be four separate aggregates in Figure 2e, there is actually only one aggregate, which crosses the periodic boundary conditions. In contrast, the oil + HMC system formed many smaller oil aggregates, which can be seen in Figure 2f. We speculate that the HMCs help stabilize the smaller oil aggregates and prevent them from coalescing via the modification chains anchoring into the oil droplets and the chitosan backbone remaining on the perimeter of each droplet. We believe that a combination of repulsion between the chitosan and oil spheres and steric hindrance of the chitosan backbone covering the oil aggregates prevents the oil from coalescing as much as in systems without HMCs. Once the modification chains of the HMCs penetrate the oil aggregates, the motion of the chitosan backbone is restricted because it is pinned to the oil aggregates at multiple locations. Therefore,

the backbone acts to block new oil chains from joining the aggregate.

The oil surface area over time was calculated to determine the efficacy of the HMCs in preventing oil aggregation; larger oil surface areas mean less aggregation. The purpose of using HMCs is to maximize the oil surface area over time, therefore providing more surface area for hydrocarbon-degrading bacteria to naturally degrade the oil before it forms a surface slick. Figure 3 shows the oil SASA over time at $\phi_{\text{hmc}} = 0.5$ for HMCs

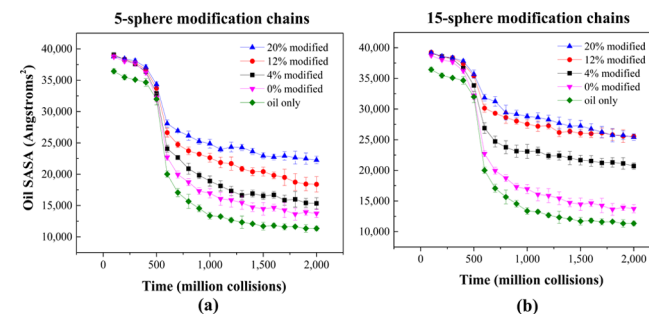


Figure 3. Effect of HMC modification density on the ability of HMCs with (a) 5- and (b) 15-sphere modification chains to prevent oil aggregation for $\phi_{\text{hmc}} = 0.5$.

with (a) 5-sphere and (b) 15-sphere modification chains and various modification densities. The green line in both plots shows the oil SASA over time without any HMCs in the system, while the pink line shows the oil SASA in a system with unmodified chitosan. The black, red, and blue lines show the oil SASA over time in systems of HMCs that are 4, 12, and 20% modified, respectively. It can be seen that the oil SASA decreases over time in systems with and without HMCs because small oil aggregates coalesce into larger ones. Increasing the modification density increases the oil SASA at the end of the simulations at all modification densities tested for HMCs with 5-sphere modification chains. A somewhat different trend occurs for HMCs with 15-sphere modification chains. The oil SASA increases with increasing modification density from 4 to 12% but reaches a plateau thereafter; the oil SASA is nearly identical at modification densities of 12 and 20%. One possible explanation for the plateau is that the total HMC concentration is so high that it causes the oil droplets to be saturated with HMC molecules. To test this hypothesis, we performed simulations at lower HMC concentrations of $\phi_{\text{hmc}} = 0.35$ and $\phi_{\text{hmc}} = 0.2$. The results from these simulations will be discussed in the next paragraph. The conclusion that we draw from Figure 3 is that HMCs with long modification chains are more effective at lower modification densities than HMCs with short modification chains. We speculate that the longer modification chains not only penetrate more deeply into the oil aggregates but also have a higher probability of interacting with more oil chains before they have the chance to aggregate due to their extended "reach". The increased interaction between long modification chains and oil disrupts oil chain packing, therefore making it more difficult for oil chains to form spherical droplets with minimum surface area. To ensure that 2 billion collisions was enough to capture the majority of the aggregation behavior, we also ran some sample simulations for 4 billion collisions and determined that the oil SASA decreased by less than 5% between 2 and 4 billion collisions. Therefore, we ended our simulations at 2 billion collisions.

Figure 4 summarizes the efficacy of different HMC architectures at concentrations of $\phi_{\text{hmc}} = 0.5$, 0.35, and 0.2,

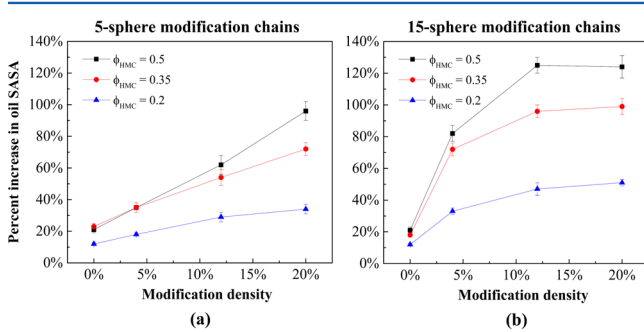


Figure 4. Percent increase in oil SASA for HMCs with (a) 5- or (b) 15-sphere modification chains and varying modification density.

by plotting the percent increase in oil SASA resulting from (a) 5-sphere and (b) 15-sphere modification chain HMCs over the oil SASA without HMCs present at the end of the simulations at various modification densities. Figure 4 confirms that there is a relatively linear trend in the percent increase in oil SASA with increasing modification density for HMCs with 5-sphere modification chains. In contrast, as we saw from Figure 3, there is clearly a modification density of HMCs with 15-sphere modification chains, above which the percent increase in oil surface area remains essentially unchanged, even at the lowest HMC concentration tested ($\phi_{\text{hmc}} = 0.2$). This shows that the saturation phenomenon persists regardless of the HMC concentration, and we can therefore conclude that it is unnecessary to use a modification density above 12% for HMCs with 15-sphere modification chains at any HMC concentration. To determine the optimum modification density with 5-sphere modification chains, we would need to increase the modification density further; however, this would far exceed the modification densities used in experiments.

Oil aggregate size distributions were calculated to quantify the number of oil aggregates of each size at different times throughout the simulation. These distributions were averaged over time and over five simulation replicates. Data reported at 0.75, 1.25, and 2 billion collisions was averaged from 0.7–0.8, 1.2–1.3, and 1.9–2.0 billion collisions, respectively (with data collected every 0.01 billion collisions). Oil chains were defined to be in a cluster if any spheres on two separate chains were within each other's square-wells. If an oil cluster contained five or more oil chains, it was considered an aggregate. Figure 5 compares the oil aggregate size distributions for simulations of 20% modified HMCs with 5- or 15-sphere modification chains at $\phi_{\text{hmc}} = 0.5$ at various times throughout the simulation. The number of small aggregates (50 chains or less) significantly decreases over time as the aggregates coalesce. This behavior reflects what happens in an oil spill scenario, where small oil droplets coalesce into a slick on the ocean surface. Figure 5 also shows that the aggregate size distributions using 5- or 15-sphere modification chains differ significantly for 20% modified HMCs. There are nearly twice as many small oil aggregates (50 chains or less) for HMCs with 5-sphere modification chains as there are for 15-sphere modification chains after 1.25 billion collisions. By the end of the simulations, the aggregate size distribution is skewed to favor smaller aggregates for 5-sphere modification chains but is more evenly distributed for 15-sphere modification chains. Therefore, at this high modification density, HMCs with short modification chains result in many

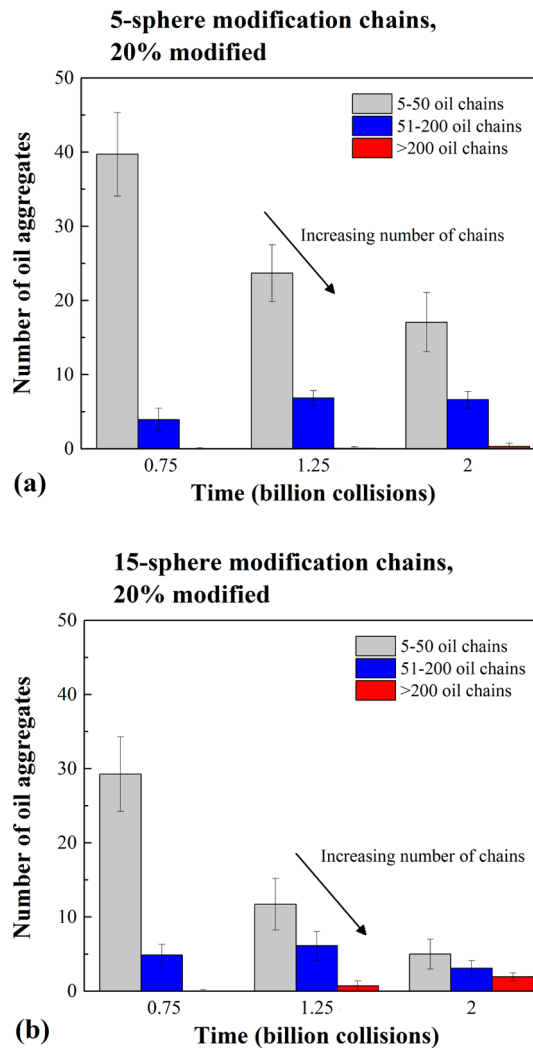


Figure 5. Oil aggregate size distributions over time using 20% modified HMCs with (a) 5- or (b) 15-sphere modification chains at $\phi_{\text{hmc}} = 0.5$.

small aggregates, while HMCs with long modification chains result in a few large oil aggregates.

Oil aggregate size distributions were also calculated for the other ϕ_{hmc} to determine if the trends just described also hold in these cases. Figure 6 shows the oil aggregate size distributions at the end of simulations of 20% modified HMCs with 5- or 15-sphere modification chains at $\phi_{\text{hmc}} = 0.5$, 0.35, and 0.2. (Note that, unlike Figure 5, these distributions are all calculated at the end of simulations and not at different time points throughout the simulations.) The aggregate size distributions at $\phi_{\text{hmc}} = 0.5$ and 0.35 show similar behavior to that seen in Figure 5, where short modification chains lead to more small oil aggregates and long modification chains lead to more large oil aggregates. At $\phi_{\text{hmc}} = 0.2$, there is no distinguishable difference in the oil aggregate size distribution between HMCs with short or long modification chains because there were too few HMCs to make a significant impact on the oil aggregate size distribution. However, even low concentrations of HMCs lead to more small aggregates than systems without HMCs, which form a single large aggregate by the end of the simulations. Therefore, the HMCs are beneficial in reducing oil aggregation even at the lowest concentrations tested.

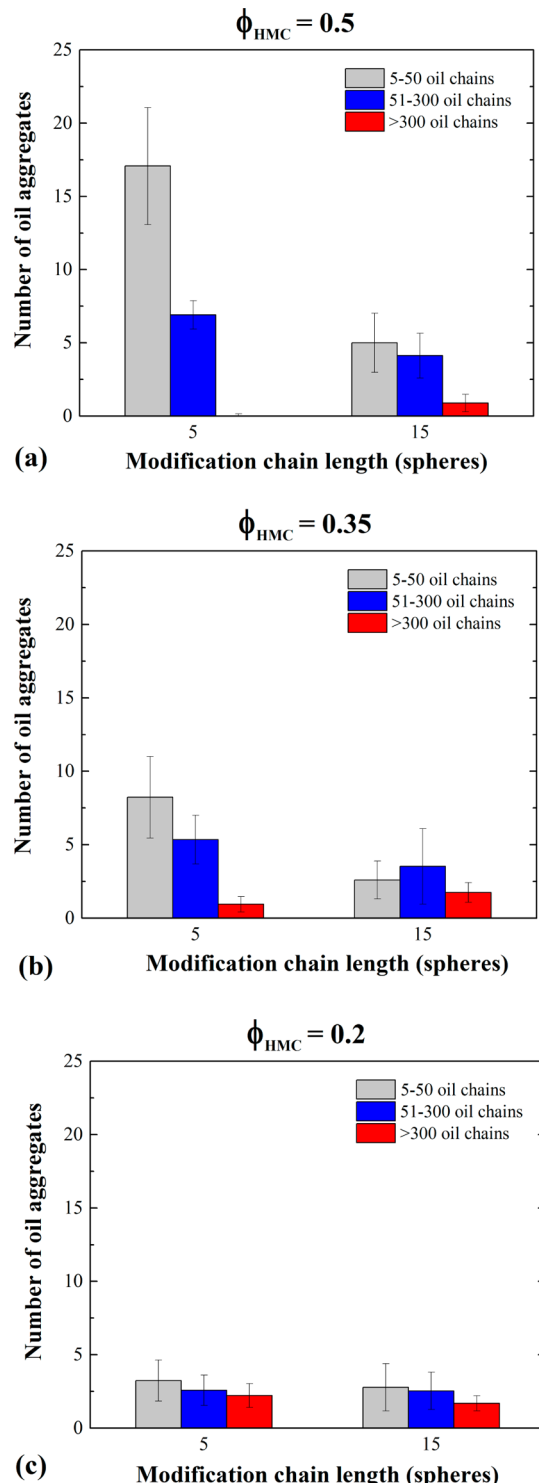


Figure 6. Oil aggregate size distributions at the end of simulations using 20% modified HMCs with 5- or 15-sphere modification chains with $\phi_{\text{hmc}} =$ (a) 0.5, (b) 0.35, and (c) 0.2.

In addition to influencing the size distribution of oil aggregates, penetration of the hydrophobic modification chains affects the shape of the oil aggregates. Figure 7 compares snapshots of the system at the end of simulations using 20% modified HMCs with 5- and 15-sphere modification chains with those of a system containing oil only to get a qualitative perspective on the shape of the oil aggregates in each system. Figure 7a shows a system containing oil only, while parts b and

c of Figure 7 show systems with 5- and 15-sphere modification chain HMCs, respectively, at $\phi_{\text{hmc}} = 0.5$. The HMCs are removed from the snapshots to more clearly see the oil aggregates. The oil chains that are not in aggregates are in yellow, and the largest oil aggregates in the system are in different colors. Note that the different colors are used only to distinguish between unique aggregates and are no indication of size or geometry of the aggregates. The system without HMCs forms one large aggregate that includes nearly all of the oil chains in the system. The oil aggregates in the system containing HMCs with 5-sphere modification chains are relatively symmetrical and tightly packed. In contrast, the oil aggregates in the system containing HMCs with 15-sphere modification chains are asymmetrical and stretched in one or more directions, helping to increase the oil SASA. Note that, although the green aggregate in the snapshot of the system containing 15-sphere modification chains appears spherical, it is significantly stretched in the direction going into the page. The asymmetry in oil aggregate shape is most noticeable at high modification densities, because there are more modification chains present to penetrate each oil droplet. Figure 7c reveals many pores in the oil aggregates, providing visual evidence of the ability of long modification chains to penetrate into the aggregates. In contrast, very few pores are visible in the oil aggregates in Figure 7b, showing the inability of the short modification chains to penetrate deeply into the oil aggregates. We would like to clarify that the pores observed in Figure 7c are merely the voids left by removing the HMCs from the snapshot. Their presence demonstrates how effectively the long modification chains penetrate the oil aggregates.

Oil aggregate asphericity was calculated to get a more quantitative measure of the shape of oil aggregates. Asphericity gives more insight into the shape of aggregates than the radius of gyration because it shows if the aggregate is elongated in any direction. Table 2 shows the average values of asphericity for oil aggregates in systems of HMCs with various modification densities and modification chain lengths at $\phi_{\text{hmc}} = 0.5$. There is little variation in oil aggregate asphericity with modification density for 5-sphere modification chains, but there is a noticeable variation with modification density for 15-sphere modification chains. Increasing the modification density from 4 to 20% for 15-sphere modification chains increases the asphericity by approximately 50%, meaning that the oil aggregates become more elongated. Not only does this confirm the behavior observed in Figure 7, but it also provides an explanation for why HMCs with 5-sphere modification chains lead to a greater number of small aggregates but still result in a lower oil surface area. As oil chains coalesce, spherical droplets form to maximize the number of favorable oil–oil contacts, resulting in the minimum possible surface area. Therefore, even though there are a greater number of small aggregates with 5-sphere modification chains, all of the aggregates minimize their surface area by taking on a spherical shape. Although there are fewer (and larger) aggregates in systems with 15-sphere modification chains, the HMCs more effectively penetrate into the oil aggregates, elongating the aggregates, and creating more oil surface area.

To prove that long modification chains more effectively penetrate into the oil aggregates, we calculated the percentage of modification spheres interacting with oil spheres in systems of HMCs with 5- and 15-sphere modification chains. The percentage of modification spheres interacting with oil spheres over time for 20% modified HMCs at $\phi_{\text{hmc}} = 0.5$ can be seen in

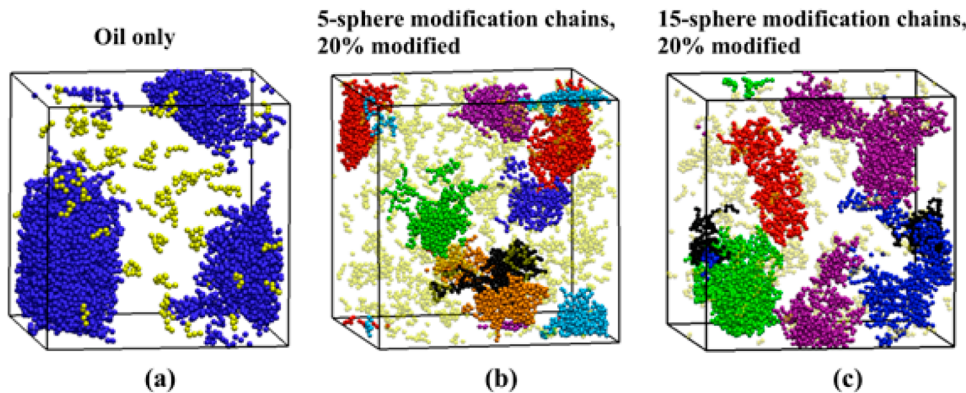


Figure 7. Snapshots of oil aggregates at the end of simulations containing (a) only oil, (b) 20% modified HMCs with 5-sphere modification chains, and (c) 20% modified HMCs with 15-sphere modification chains. Systems with HMCs were at $\phi_{\text{hmc}} = 0.5$.

Table 2. Average Asphericity of Oil Aggregates for Systems of HMCs with Various Modification Densities and Modification Chain Lengths for $\phi_{\text{hmc}} = 0.5$

modification density	5-sphere modification chains	15-sphere modification chains
4%	0.17 ± 0.18	0.21 ± 0.16
12%	0.19 ± 0.16	0.33 ± 0.19
20%	0.18 ± 0.14	0.33 ± 0.17

Figure 8. Two spheres are considered to be interacting if they are within each other's square-wells, therefore experiencing an

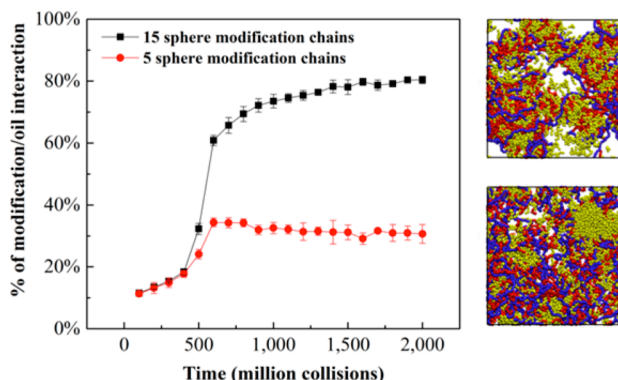


Figure 8. Percentage of modification spheres interacting with oil spheres during simulations with 20% modified HMCs with 5- and 15-sphere modification chains.

attractive interaction for each other. Snapshots of systems with 15-sphere modification chain HMCs (top) and 5-sphere modification chain HMCs (bottom) at the end of simulations are also shown to illustrate the difference in the interaction of short and long modification chains with oil aggregates. Figure 8 shows that there is a drastic difference in the percentage of modification spheres interacting with oil spheres for the two different modification chain lengths. By the end of the simulations, approximately 80% of the modification spheres interact with oil spheres for HMCs with 15-sphere modification chains, while only about 30% interact with oil for HMCs with 5-sphere modification chains. The increased ability of long modification chains to penetrate oil aggregates is illustrated in the snapshots to the right of the chart in Figure 8. The top snapshot (15-sphere modification chains) shows good mixing between the modification spheres and oil spheres, while the

bottom snapshot (5-sphere modification chains) shows separate oil and modification domains with no significant penetration of the modification chains into the oil aggregates. The percentage of modification spheres interacting with oil spheres is nearly identical regardless of modification density (data not shown).

Modification chain length and modification density not only affect HMCs' interactions with oil but also affect HMCs' interaction with each other. Figure 9 shows snapshots of systems of 20% modified HMCs at the end of simulations with 5- and 15-sphere modification chains at $\phi_{\text{hmc}} = 0.2$, as well as a snapshot at the end of a simulation using unmodified chitosan. (Note that oil was present in each of these simulations but has been removed to allow easier visualization of the HMC network.) Each system contains the same total number of HMC spheres (or unmodified chitosan spheres in Figure 9a). The snapshots in Figure 9 show that varying the modification chain lengths results in different HMC network architectures. The longer "reach" of the 15-sphere modification chains causes the modification chains to dominate network formation, as indicated by the large hydrophobic clusters in red. The shorter "reach" of the 5-sphere modification chains causes the chitosan backbone to dominate network formation, meaning that the orientation of the molecules within the network is more controlled by the chitosan backbone stiffness than by the hydrophobic interaction between modification chains. The network formed by the unmodified chitosan is also controlled by chitosan stiffness due to the lack of hydrophobic interactions by modification chains. The strong association of long modification chains shows how long modification chain HMCs lead to more elongated oil aggregates.

At this point, the effectiveness of HMCs as oil stabilizers has been analyzed using a number of techniques; however, one important question remains. Are HMCs with few long modification chains better at preventing oil aggregation than HMCs with many short modification chains if the total number of modification spheres is the same? To determine if the architecture plays a role in oil stabilization, it is necessary to compare two different HMC architectures with the same total number of chitosan and modification spheres per molecule. This determines if stabilizing oil droplets depends on more than just the total number of modification spheres in the system. Therefore, we compared simulations of 4% modified HMCs with 15-sphere modification chains and 12% modified HMCs with 5-sphere modification chains in oil at $\phi_{\text{hmc}} = 0.5$. The HMCs that were 4% modified with 15-sphere modification

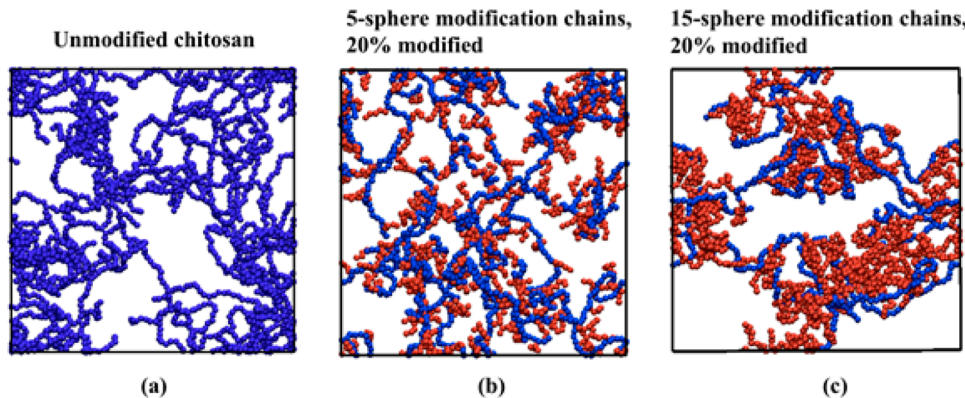


Figure 9. Snapshots of networks formed by (a) unmodified chitosan, (b) 20% modified HMCs with 5-sphere modification chains, and (c) 20% modified HMCs with 15-sphere modification chains. Chitosan spheres are in blue, and modification spheres are in red.

chains had two modification chains on the chitosan backbone, while the HMCs that were 12% modified with 5-sphere modification chains had six modification chains on the chitosan backbone. However, both HMCs had the same total number of chitosan spheres (50) and modification spheres (30) per molecule. The final oil SASA using HMCs with 15-sphere modification chains was 12% higher than the oil SASA using HMCs with 5-sphere modification chains (data not shown). This is consistent with the behavior discussed previously where longer modification chains led to a larger oil SASA, and also shows that the HMC architecture does play a role in oil dispersion, even for HMCs with the same number of modification spheres.

The oil aggregate size distribution for these two HMC architectures was calculated to compare the number and size of oil aggregates formed. This can be seen in Figure 10, which shows that HMCs with long modification chains result in fewer small aggregates (<50 chains) than HMCs with short modification chains even though the total number of spheres for the two HMCs is the same. We also observed the formation of slightly more large aggregates (>200 chains) with long modification chain HMCs than with short modification chain HMCs. These results are in agreement with the previously mentioned aggregate size distributions, where long modification chains promoted the formation of larger oil aggregates. From these results, we can conclude that HMC architecture does affect both the oil SASA and the size distribution of oil aggregates, and that the HMC efficacy is dependent on more than just the total number of modification spheres in the system.

To ensure that the increase of oil SASA in systems containing HMCs was not simply due to the HMCs “getting in the way” of the oil chains, the interaction energies between the various species were systematically set to zero one at a time, to pinpoint the important interactions. The rationale for this exercise is that, if the HMCs simply prevented oil aggregation because they took up space in the simulation box, setting attractive/repulsive interactions between HMCs and oil to zero would result in approximately the same oil SASA over time as simulations with all of the interactions accounted for between the HMCs and oil. Note that the attractive interaction between oil spheres is always present to ensure that the oil aggregates in all simulations. Four total cases were tested to determine the most important interaction energies: (1) no interactions were set to zero, (2) chitosan backbone interactions were set to zero,

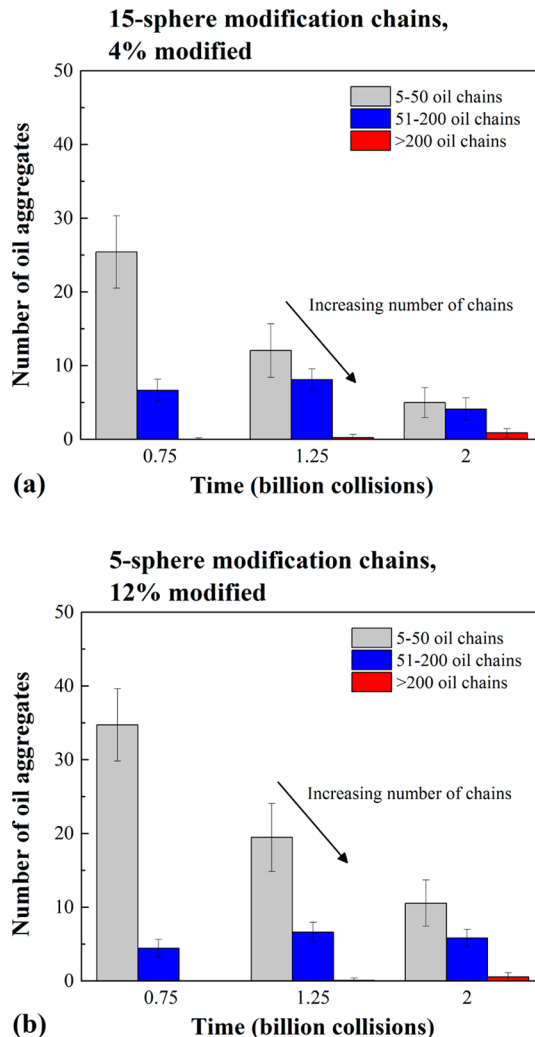


Figure 10. Oil aggregate size distributions comparing systems of HMCs with (a) a few long modification chains and (b) many short modification chains at $\phi_{\text{hmc}} = 0.5$.

(3) modification chain interactions were set to zero, (4) all interaction energies were set to zero.

Table 3 shows the percent increases in oil SASA over systems of oil only (defined in eq 2) for the four cases described above. This data confirms that the interaction between modification chains and oil chains controls the ability of HMCs to prevent

Table 3. Percent Increase in Oil SASA in Systems of 4% Modified HMCs with 5- and 15-Sphere Modification Chains at $\phi_{\text{hmc}} = 0.5$ over Systems of Oil Only

case no.	HMC interactions set to zero	5-sphere modification chains	15-sphere modification chains
1	none	35.3%	83.6%
2	backbone	31.1%	75.3%
3	modification	20.1%	18.2%
4	all	10.5%	12.1%

oil aggregation because there is only a slight difference in the oil SASA between the case 2 systems (backbone interactions set to zero) and the case 1 systems (no interactions set to zero) for both 5-sphere and 15-sphere modification chains. It is somewhat surprising to find that the modification chain interactions are the most important interactions for HMCs with 5-sphere modification chains, especially after determining that only about 30% of the modification spheres interact with the oil. However, this supports the argument that the modification chains act to anchor the oil droplets to the chitosan backbone, therefore restricting their movement and preventing aggregation even though they cannot deeply penetrate the oil droplets. Comparison of the case 3 systems (modification interactions set to zero) and the case 1 systems (no interaction energies set to zero) shows that the chitosan backbone interactions play only a minor role in preventing oil aggregation because the increase in oil SASA drastically decreases when only backbone interactions are present. The backbone interactions most likely play a minor role because our simulations use an implicit solvent model; therefore, there are no polar water molecules for the chitosan spheres to be attracted to. We also showed that the efficacy of the HMC stabilizers is not purely dependent on the excluded volume interactions between the HMCs and oil. In fact, excluded volume interactions alone play a minor role in the HMC's ability to prevent oil aggregation because the oil SASA at the end of the case 4 simulations (all interaction energies set to zero) is only 10–12% larger than in systems containing oil only.

CONCLUSIONS

We have presented the results of discontinuous molecular dynamics simulations aimed at determining the efficacy of HMCs as oil stabilizers and the key parameters that govern their ability to prevent oil aggregation. HMCs with modification chain lengths of 5 and 15 spheres and modification densities of 4, 12, and 20% were considered. Throughout the course of the simulations, the extent of oil aggregation was monitored in a number of ways for systems with different HMC architectures. First we monitored the oil SASA throughout the course of simulations to get a “big picture” look at the effectiveness of the HMCs, where larger oil SASAs indicate more effective HMCs. This analysis determined if the HMCs were effective or not but did not give insight into how they prevented oil aggregation. We concluded that all HMCs tested led to larger oil SASA over time than systems without HMCs, for systems starting in a random initial configuration of oil and HMC molecules in the simulation box. Additionally, increasing the modification chain length and modification density led to an increase in the oil SASA. There did appear to be a saturation modification density above which there was no increase in oil SASA for the 15-sphere

modification chains, as the HMCs that were 12 and 20% modified had nearly identical oil SASA. This shows that it is unnecessary to exceed a modification density of 12% when using the 15-sphere modification chains. However, there was an increase in oil SASA with increasing modification density for HMCs with 5-sphere modification chains for all modification densities tested.

Next we looked at the oil aggregate size distributions for systems of HMCs with various modification densities and modification chain lengths. This analysis revealed that HMCs with long modification chains led to fewer and larger oil aggregates than systems with short modification chains. This contradicted the results we expected, given that HMCs with long modification chains had larger oil SASAs than HMCs with short modification chains. One would have expected that an increase in oil SASA would coincide with a greater number of small oil aggregates rather than fewer large oil aggregates. The only way it would have been possible to have a larger oil surface area and larger oil aggregates would be for the aggregates to be stretched. To test this hypothesis, we first looked at snapshots of the oil phase at the end of simulations to get a qualitative understanding of the oil aggregate shape. It was clear from these snapshots that the oil aggregates in systems of HMCs with long modifications were indeed more stretched and aspherical than oil aggregates in a system with short modification chain HMCs. We concluded that the oil aggregate asphericity for HMCs with 5-sphere modification chains does not vary significantly with increasing modification density, while that for 15-sphere modification chains increases by approximately 50% going from the lowest to highest modification densities. The longer modification chains more effectively penetrate into the oil aggregates, deforming their shape.

Finally we determined that the interaction between the modification chains and the oil chains was the most important interaction in the HMCs preventing oil aggregation. The oil SASA in a system containing HMCs with only modification chain interactions was very similar to that of a system with all HMC interactions. We believe that short modification chain HMCs prevent oil aggregation by anchoring the chitosan backbones to the oil aggregates, in turn restricting the movement of the aggregates and preventing aggregation. In contrast, we have shown that the long modification chain HMCs prevent aggregation by penetrating deeply into the aggregates and preventing them from forming small, spherical droplets.

In conclusion, we have gained insight into the optimum HMC architectures for preventing oil aggregation. Our results conceptually agree with the experimental work of Venkataraman and co-workers¹⁸ and can be used to help design effective HMC oil stabilizers. One way that our simulations differ from the work of Venkataraman and co-workers is that we did not include Corexit in the system. Corexit is primarily used to break up oil into smaller droplets. In a way, we accounted implicitly for addition of Corexit by starting our simulations in a random initial configuration with oil molecules already broken up. If we were to include Corexit in the simulations, the efficacy of HMCs might increase due to electrostatic attraction between the cationic chitosan monomers and the anionic surfactant, dioctyl sodium sulfosuccinate (DOSS), present in Corexit. This might allow the HMCs to adhere more strongly to the oil droplets and possibly travel to the oil/water interface more quickly. We plan to include Corexit in a follow-up study. In its current state, our model can be easily applied to study different

chitosan molecular weights, different types of modification chains, and different HMC concentrations. We are currently extending our model to include more details about the chitosan backbone such as the degree of acetylation and surface charge, making the model more universally applicable to a variety of conditions.

Although our model of an oil/HMC system has many advantages for qualitative study of HMCs as oil dispersant additives, it has several limitations. The first limitation is that we used an implicit solvent approach, which does not accurately represent the diffusion of molecules or hydrodynamics. Because there are no water molecules to collide with the solute, the solute molecules travel more quickly through the simulation box than they would in the presence of water. The second limitation is that it is difficult to make a direct correlation between the reduced temperature in the simulation and real temperature. Values of the reduced temperature and interaction energies were chosen to make the oil aggregate gradually over the course of the simulation (several hundred million collisions) as opposed to being derived via multiscale modeling of atomistic simulations. Therefore, the chosen temperature is not directly related to the real temperature, as would be the case in atomistic simulations. The third limitation of this method is that we do not have a way to correlate simulation time to real time because molecules move in a straight line in a vacuum between collisions, rather than traveling through solvent. In order to correlate our results to a real time scale, we would have to compare the time it takes for a specific molecular mechanism to occur in experiments and simulations. Unfortunately, we are unable to identify a mechanism that would be distinguishable in both experiments and simulations to compare the time scales.

AUTHOR INFORMATION

Corresponding Author

*E-mail: hall@ncsu.edu. Phone: 919-515-3571. Fax: 919-515-3463.

Author Contributions

The manuscript was written through equal contributions of all authors. All authors have given approval to the final version of the manuscript.

Notes

The authors declare no competing financial interest.

ACKNOWLEDGMENTS

This work was supported by the GAANN Computational Science Fellowship and the Gulf of Mexico Research Initiative (GOMRI). This work was also supported in part by the NSF's Research Triangle MRSEC, DMR-1121107.

ABBREVIATIONS

HMC, hydrophobically modified chitosan; DMD, discontinuous molecular dynamics; VMD, visual molecular dynamics

REFERENCES

- (1) Kujawinski, E. B.; Soule, M. C. K.; Valentine, D. L.; Boysen, A. K.; Longnecker, K.; Redmond, M. C. Fate of Dispersants Associated with the Deepwater Horizon Oil Spill. *Environ. Sci. Technol.* **2011**, *45*, 1298–1306.
- (2) Piatt, J.; Lensink, C.; Butler, W.; Kendziorek, M.; Nysewander, D. Immediate Impact of the Exxon Valdez Oil-Spill on Marine Birds. *Auk* **1990**, *107*, 387–397.
- (3) Baelum, J.; Borlin, S.; Chakraborty, R.; Fortney, J.; Lamendella, R.; Mason, O.; Auer, M.; Zemla, M.; Bill, M.; Conrad, M.; et al. Deep-Sea Bacteria Enriched by Oil and Dispersant from the Deepwater Horizon Spill. *Environ. Microbiol.* **2012**, *14*, 2405–2416.
- (4) Thibodeaux, L. J.; Valsaraj, K. T.; John, V. T.; Papadopoulos, K. D.; Pratt, L. R.; Pesika, N. S. Marine Oil Fate: Knowledge Gaps, Basic Research, and Development Needs; A Perspective Based on the Deepwater Horizon Spill. *Environ. Eng. Sci.* **2011**, *28*, 87–93.
- (5) Zahed, M.; Aziz, H.; Isa, M.; Mohajeri, L.; Mohajeri, S.; Kutty, S. Kinetic Modeling and Half Life Study on Bioremediation of Crude Oil Dispersed by Corexit 9500. *J. Hazard. Mater.* **2011**, *185*, 1027–1031.
- (6) Leahy, J.; Colwell, R. Microbial Degradation of Hydrocarbons in the Environment. *Microbiol. Rev.* **1990**, *54*, 305–315.
- (7) Rinaudo, M. Chitin and Chitosan: Properties and Applications. *Prog. Polym. Sci.* **2006**, *31*, 603–632.
- (8) Majeti, N. V.; Kumar, R. A Review of Chitin and Chitosan Applications. *React. Funct. Polym.* **2000**, *46*, 1–27.
- (9) Aranaz, I.; Harris, R.; Heras, A. Chitosan Amphiphilic Derivatives. Chemistry and Applications. *Curr. Org. Chem.* **2010**, *14*, 308–330.
- (10) Kumar, R.; Muzzarelli, A.; Muzzarelli, C.; Sashiwa, H.; Domb, A. J. Chitosan Chemistry and Pharmaceutical Perspectives. *Chem. Rev.* **2004**, *104*, 6017–6084.
- (11) Martino, A.; Sittinger, M.; Risbud, M. Chitosan: A Versatile Biopolymer for Orthopaedic Tissue-Engineering. *Biomaterials* **2005**, *26*, 5983–5990.
- (12) Berger, J.; Reist, M.; Mayer, J. M.; Felt, O.; Gurny, R. Structure and Interactions in Chitosan Hydrogels Formed by Complexation Or Aggregation for Biomedical Applications. *Eur. J. Pharm. Biopharm.* **2004**, *57*, 35–52.
- (13) Chen, Y.; Javvaji, V.; MacIntire, I.; Raghavan, S. Gelation of Vesicles and Nanoparticles using Water-Soluble Hydrophobically Modified Chitosan. *Langmuir* **2013**, *29*, 15302–15308.
- (14) Dennis, J.; Meng, Q.; Zheng, R.; Pesika, N.; McPherson, G.; He, J.; Ashbaugh, H.; John, V.; Dowling, M.; Raghavan, S. Carbon Microspheres as Network Nodes in a Novel Biocompatible Gel. *Soft Matter* **2011**, *7*, 4170–4173.
- (15) Ashmore, M.; Hearn, J.; Karpowicz, F. Flocculation of Latex Particles of Varying Surface Charge Densities by Chitosans. *Langmuir* **2001**, *17*, 1069–1073.
- (16) Rojas-Reyna, R.; Schwarz, S.; Heinrich, G.; Petzold, G.; Schütze, S.; Bohrisch, J. Flocculation Efficiency of Modified Water Soluble Chitosan Versus Commonly used Commercial Polyelectrolytes. *Carbohydr. Polym.* **2010**, *81*, 317–322.
- (17) Bratskaya, S.; Avramenko, V.; Schwarz, S.; Philippova, I. Enhanced Flocculation of Oil-in-Water Emulsions by Hydrophobically Modified Chitosan Derivatives. *Colloids Surf., A* **2006**, *275*, 168–176.
- (18) Venkataraman, P.; Tang, J.; Frenkel, E.; McPherson, G.; He, J.; Raghavan, S.; Kolesnichenko, V.; Bose, A.; John, V. Attachment of a Hydrophobically Modified Biopolymer at the Oil-Water Interface in the Treatment of Oil Spills. *ACS Appl. Mater. Interfaces* **2013**, *5*, 3572–3580.
- (19) Lyatskaya, Y.; Gersappe, D.; Balazs, A. Effect of Copolymer Architecture on the Efficiency of Compatibilizers. *Macromolecules* **1995**, *28*, 6278–6283.
- (20) Lyatskaya, Y.; Balazs, A. Using Copolymer Mixtures to Compatibilize Immiscible Homopolymer Blends. *Macromolecules* **1996**, *29*, 7581–7587.
- (21) Gersappe, D.; Harm, P.; Irvine, D.; Balazs, A. Contrasting the Compatibilizing Activity of Comb and Linear Copolymers. *Macromolecules* **1994**, *27*, 720–724.
- (22) de Jong, J.; Subbotin, A.; ten Brinke, G. Spontaneous Curvature of Comb Copolymers Strongly Adsorbed at a Flat Interface: A Computer Simulation Study. *Macromolecules* **2005**, *38*, 6718–6725.
- (23) Israels, R.; Foster, D.; Balazs, A. Designing Optimal Comb Copolymers: AC and BC Combs at an A/B Interface. *Macromolecules* **1995**, *28*, 218–224.
- (24) Potemkin, I.; Khokhlov, A.; et al. Spontaneous Curvature of Comblike Polymers at a Flat Interface. *Macromolecules* **2004**, *37*, 3918–3923.

- (25) Vasilevskaya, V.; Klochkov, A.; Khalatur, P.; Khokhlov, A.; ten Brinke, G. Microphase Separation within a CombCopolymer with Attractive Side Chains: A Computer Simulation Study. *Macromol. Theory Simul.* **2001**, *10*, 389–394.
- (26) Malik, R.; Hall, C. K.; Genzer, J. Protein-Like Copolymers (PLCs) as Compatibilizers for Homopolymer Blends. *Macromolecules* **2010**, *43*, 5149–5157.
- (27) Malik, R.; Hall, C. K.; Genzer, J. Effect of Copolymer Compatibilizer Sequence on the Dynamics of Phase Separation of Immiscible Binary Homopolymer Blends. *Soft Matter* **2011**, *7*, 10620–10630.
- (28) Malik, R.; Hall, C. K.; Genzer, J. Phase Separation Dynamics for a Polymer Blend Compatibilized by Protein-Like Copolymers: A Monte Carlo Simulation. *Macromolecules* **2011**, *44*, 8284–8293.
- (29) Smith, S.; Hall, C.; Freeman, B. Molecular Dynamics for Polymeric Fluids using Discontinuous Potentials. *J. Comput. Phys.* **1997**, *134*, 16–30.
- (30) Wang, Z.; Hollebone, B. P.; Fingas, M.; Fieldhouse, B.; Sigouin, L.; Landriault, M.; Smith, P.; Noonan, J.; Thouin, G. *Characteristics of Spilled Oils, Fuels, and Petroleum Products: 1. Composition and Properties of Selected Oils*; 2003; pp 1–286.
- (31) Rapaport, D. C. Molecular Dynamics Simulation of Polymer Chains with Excluded Volume. *J. Phys. A* **1978**, *11*, L213–L217.
- (32) Rapaport, D. C. Molecular Dynamics Study of a Polymer Chain in Solution. *J. Chem. Phys.* **1979**, *71*, 3299–3303.
- (33) Alder, B.; Wainwright, T. Studies in Molecular Dynamics 0.1. General Method. *J. Chem. Phys.* **1959**, *31*, 459–466.
- (34) Andersen, H. Molecular-Dynamics Simulations at Constant Pressure and-Or Temperature. *J. Chem. Phys.* **1980**, *72*, 2384–2393.
- (35) Gaspari, G.; Rudnick, J. The Shapes of Random Walks. *Science* **1987**, *237*, 384–389.
- (36) Janke, W.; Arkin, H. Gyration Tensor Based Analysis of the Shapes of Polymer Chains in an Attractive Spherical Cage. *J. Chem. Phys.* **2013**, *138*, 1–8.